Journal of Navigation and Port Research International Edition
Vol.32, No.9 pp. 717~722, 2008 (ISSN-1598-5725)

Gas-Flow Sensor using Optical Fiber Bragg Grating(FBG)

Joon-Hwan Shim · Seok-Je Cho** · Yung-Ho Yu*** · Kyung-Rak Sohn†*

,,***,†Division of Computer, Control and Electronic Communications Engineering, Korea Maritime University, Busan 606-791, Republic of Korea*

Abstract : *We have proposed and demonstrated an gas-flow sensor using optical fiber bragg grating(FBG). The flow sensor has no electronics and no mechanical parts in its sensing part and the structure is thus simple and immune to electromagnetic interference(EMI). The FBG sensor was consisted of the sensing element and a coil heater. The metal coil was used to supply the current to the FBG. While some currents supply to the coil, the refractive index of the FBG under the coil is changed and thus the wavelength shift of fiber optic sensor was induced. In this work, the wavelength shift according to flow-rate was experimentally studied and was used to evaluate the gas flow-rate in a gas tube. As a result, it was possible to measure the flow-rate in a linear range from 5 to 20 ℓ/min with a resolution of approximately 1 ℓ/min at the applied currents of 100 ㎃ and 120 ㎃. The measured sensitivities were 15.3 pm/ ℓ/min for 100 ㎃ and 20.2 pm/ ℓ/min for 120 ㎃.*

Key words : *Gas flow sensors, Flow sensors, Optical fiber sensors, Fiber bragg grating*

1. Introduction

Flow meters and sensors are important in various fields, such as chemical industry, oil or gas transport, water transport, among others, for monitoring or process control. Several approaches have been employed for mass flow measurement including time of flight measurement(Wu, 2002), differential pressure measurement(Svedin, 2003), and heat transfer(Oda, 2003; Kaltsas, 2002). At present, most state-of-the-art miniaturized flow sensors are fabricated using microelectromechanical systems(MEMS) technology on silicon substrates(Hung, 2000). Although MEMS flow sensors offer important advantages, such as compact size, high sensitivity, fast response time, and compatible with CMOS technologies, a number of drawbacks are also evident. The packaging of MEMS devices could be bulky. The bulky packaging limit the use of MEMS flow sensors from a number of important applications in harsh environments including cryogenic fuel flow and corrosive flow rate measurement; flow measurement in strong electromagnetic fields.

Flow measurement using optical fiber devices has also been reported based on fiber bending(Lim, 2001; Nemoto, 1998). Compared with electronic and MEMS sensors, fiber optical sensors are ideal for use in harsh environments and have a number of benefits including low manufacturing cost, high sensitivity, long lifetime, and immunity to electromagnetic fields(IMFs). An additional advantage is that the measurements of physical variables are determined by the Bragg wavelength(λ_B) shift, which is a parameter absolute and insensitive to intensity losses in the connectors or splices in the fiber. In the FBG flow sensor, the choice of the wavelength-shift detection method is very important because the noise level and the measurement bandwidth of the system are mainly determined by the detection method.

In this study, an gas-flow sensor based on hot-wire anemometry(Okamoto, 1994) is proposed and demonstrated. In order to wavelength-shift operation, a Ni-Cr coil heater is prepared to control the refractive index of a FBG. The FBG area of a fiber is inserted into the coil and is heated by a constant current source. According to the refractive index change by heating power, the resonance wavelength can be changed. At first, we explain the principle and the schematic diagram of the FBG sensor. Next, we present the experimental setup and procedure. Finally we describe experimental performances of the FBG gas-flow sensor.

2. Experiment

2.1 Principle of FBG sensor

A fiber Bragg grating is an optical fiber for which the refractive index in the core is perturbed forming a periodic or quasi-periodic index modulation profile. When a FBG experiences temperature variation, Bragg wavelength will be

* jhsim@hhu.ac.kr 051)410-4811
** sjcho@hhu.ac.kr 051)410-4344
*** yungyu@hhu.ac.kr 051)410-4345
† Corresponding author: Kyung-Rak Sohn, krsohn@hhu.ac.kr 051)410-4312

shifted by the refractive index change of a fiber and the fiber elongation. Shift in Bragg wavelength $\Delta\lambda_B$ is given by differentiating the Bragg wavelength.

$$\lambda_B = 2n_{eff}\Lambda \tag{1}$$

$$\Delta\lambda_B = 2\Delta n_{eff}\Lambda + 2n_{eff}\Delta\Lambda \tag{2}$$

where n_{eff} is the unperturbed effective refractive index, Δn_{eff} is the refractive index change, Λ is the Bragg grating period, and $\Delta\Lambda$ is the fiber elongation. Under the circumstances of no external perturbation except temperature, the first term on the right-hand side of Eq. (2) is dominant because the thermally induced fiber elongation is relatively small to the change of refractive index. Such variation of refractive index caused by the temperature change is given by (Shyu,1994; Lin, 1998).

$$\frac{\Delta n}{n} = \left(\frac{\partial n}{\partial T}\right)_\rho \frac{\Delta T}{n} + \left(\frac{\partial n}{n}\right)_T = \left(\frac{\partial n}{\partial T}\right)_\rho \frac{\Delta T}{n} - \frac{n^2}{2}\left[(P_{11}+P_{12})\epsilon_r + P_{12}\epsilon_z\right] \tag{3}$$

where P_{11} and P_{12} are the Pockels coefficients of the core and ϵ_r and ϵ_z are the radial and the axial stain in the core, respectively. The first term on the right-hand side of Eq. (3) represents variation of refractive index as a function of temperature and second term is related to the photo-elastic effect expressed in terms of the strains and Pockels coefficients. For a bare FBG, the second term on the right-hand side of Eq. (3) is negligible due to comparatively small change of the strain in the core. Note that the refractive index of a single FBG written on a commercial single-mode fiber can be partially changed by means of a local heating of the FBG region. In this study, Ni-Cr coil is used for heating the FBG. The configuration of proposed FBG flow sensor with Ni-Cr coil heater is shown in Fig. 1.

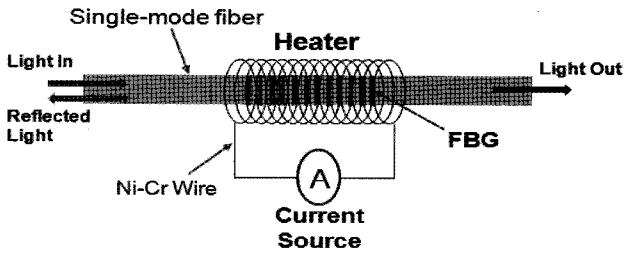

Fig. 1 Current-controlled FBG flow sensor with Ni-Cr coil heater.

2.2 Experimental Setup

In Fig. 2 is reported the experimental set-up used for the FBG gas-flow sensor characterization. It consists of a sensing FBG inserted in coil, a broadband light source, a fiber coupler, an optical spectrum analyzer, a nitrogen chamber, a flow-meter, and a flow tube. A FBG was written in a single-mode standard fiber and uniform grating with length of 27 ㎜ was used in the experiments with resonance wavelength at 1530.5 ㎚. The coil heater is made by Ni-Cr wire, which has a diameter of 200 ㎛, a length of 30 ㎜ and a resistance of 31 Ω. The flow sensor is installed in a test-flow line whose inner diameter is 10 ㎜. The spectrum is acquired in the wavelength range of 1525-1535 ㎚ with a resolution of 0.2 ㎚. A pure nitrogen gas from the bombe continuously flows in the test-flow line; the total gas flow-rate is set to 25 ℓ/min which is controlled by the calibrated flow-meter with a resolution of 1 ℓ/min. While the current is applied to the coil, if the nitrogen gas flow into the flow channel, a single resonance wavelength will be shifted due to the difference of refractive index change of the FBG. When the flow-rate is increased, the refractive index of the FBG sensor also goes down. Each resonance wavelength corresponds to each refractive index value. Thus, the

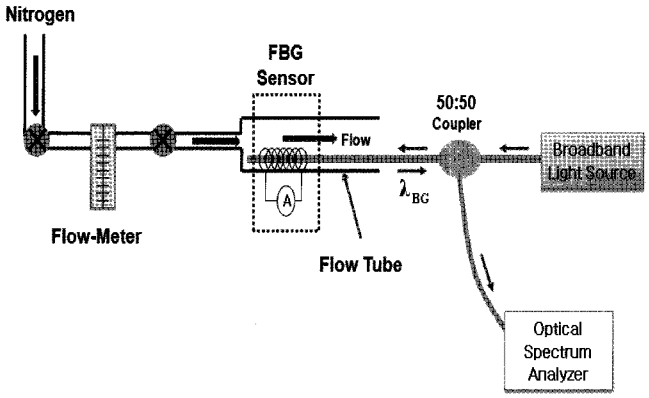

Fig. 2 Schematic diagram of the flow measurement system, which consist of white light source, optical spectrum analyzer, and the FBG sensor located in the flow channel.

Table 1 List of used experimental condition.

Applied Current (㎃) \ Flow Rate (ℓ/min)	3	4	5	10	15	20
50	●	●	●	x	x	x
80	●	●	●	x	x	x
100	●	●	●	●	●	●
120	●	●	●	●	●	●

flow-rate of gas can be sensed and measured. Table 1 summarizes the used experimental condition. The experiments are conducted three flow-rates at the applied currents of 50 and 80 ㎃ and six flow-rates at the applied currents of 100 and 120 ㎃.

3. Experimental Results and Discussion

3.1 Heat effect of the FBG sensor

The reflection spectra of the FBG in terms of the change of applied current are shown in Fig. 3. A current sources is used for generating the electrical power of the coil heater. When the current of 50 ㎃, 80 ㎃, 100 ㎃ and 120 ㎃ are supplied to the coil1, the temperature of the FBG area which is surrounded with heater is raised by the resistance heat. This operation is based on the thermally-induced refractive index change of the FBG fiber by the coil heater. Therefore, the reflection spectrum moves to the longer wavelength because the volume of the FBG sensor increases by thermal optical coefficient(13 pm/℃) and then the width of the resonant peak gradually broadens as the current increases. In this experiment, the unheated reflection peak is appeared at 1530.56 ㎚. Although the non-uniform thermal profiles slightly distort the FBG reflection spectra, the well-defined peaks of the heated FBG can be used to precisely determine temperatures of the sensors. The operation temperatures of the heated FBG sensor is similar to that used in metal-based hot-wire anemometry flow sensors.

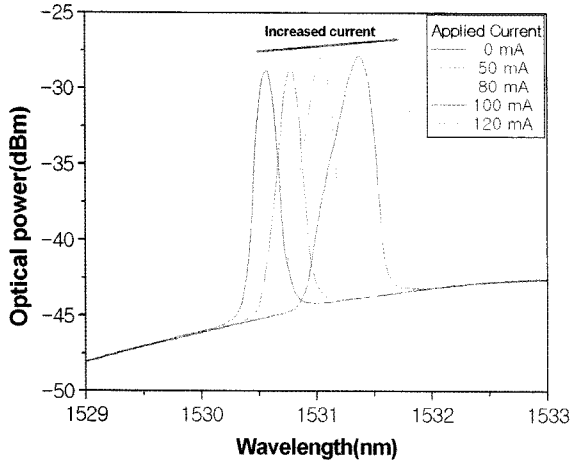

Fig. 3 Tunable spectral responses as a function of the applied current change.

Fig. 4 shows the resonance wavelength shift of the FBG sensor according to the applied current. The sensitivity of the measured FBG sensor was 12.5 pm/㎃ and the linear relationship was shown for the repeated tests. From this result, it can be used in temperature sensing applications.

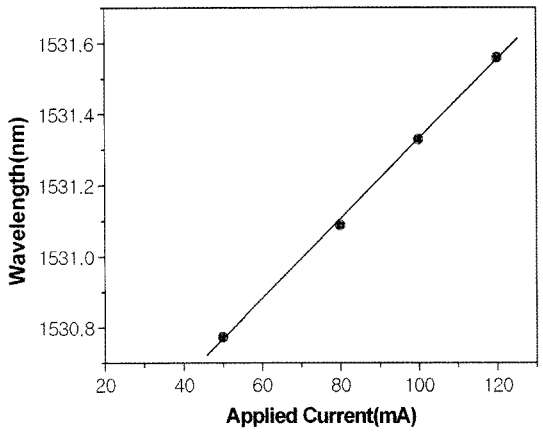

Fig. 4 A plot of the shift in resonant wavelength versus applied current.

3.2 Flow measurement of the FBG sensor

The introduction of the gas flow increases the heat removal rate from the optically heated FBG sensor and therefore reduces the temperature of the FBG sensor. This again is registered by resonance wavelength shifts of the FBG sensor shown in Fig. 5. This shows the resonance wavelength shifts of the heated FBG sensor as functions of the flow rates in the range of low flow-rates(less than 5 ℓ/min) at four applied currents of 50, 80, 100 and 120 ㎃, respectively. The results show the resonance wavelength shifts follow the nonlinear curves of the N_2 flow-rates at each applied current. The characteristics of the curves show saturation from a flow-rate of 4 ℓ/min. From this measurements, we can estimate the FBG sensor is not able to be used for low flow-rates of less than 5 ℓ/min. Fig. 6 shows the resonance wavelength shifts of the FBG sensor as a function of applied currents at three flow-rates of 3, 4 and 5 ℓ/min, respectively. It shows the higher the current, the more the sensitivity but the linear is not acceptable.

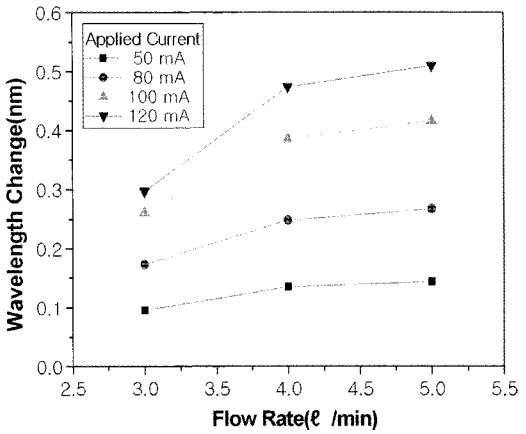

Fig. 5 Wavelength shifts against the gas flow-rates under various applied currents

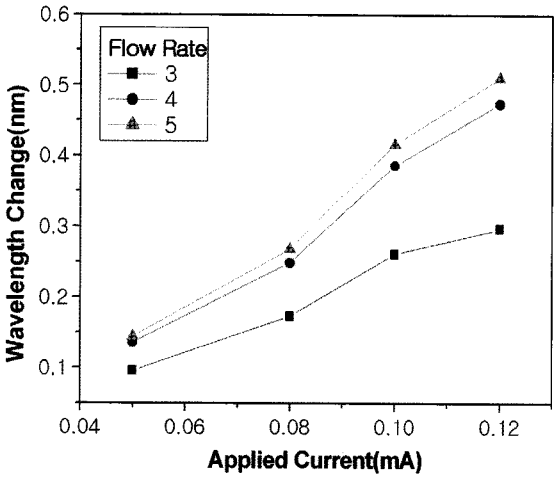

Fig. 6 Wavelength shifts against the applied currents under various gas flow-rates.

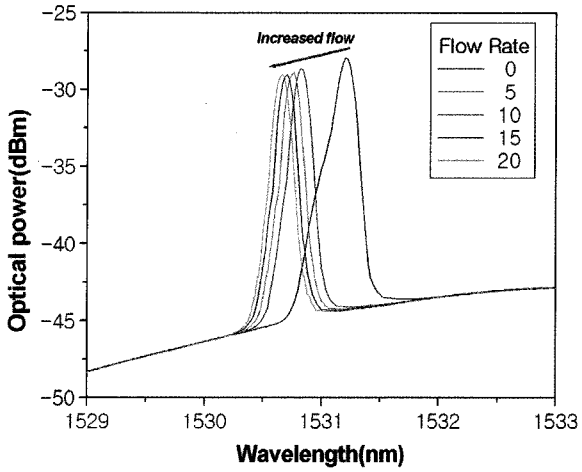

Fig. 8 Tunable spectral responses versus the gas flow-rates at the applied current of 100 ㎃.

Fig. 7 shows the resonance wavelength shifts of the heated FBG sensor as functions of the flow rates in the range from 3 to 20 ℓ/min at two applied currents of 100 and 120 ㎃, respectively. Form the results, we can estimate the curves can be divided in two parts. One is non-linear behavior at below 5 ℓ/min and another is linear behavior at above 5 ℓ/min. The gas flow experiments show that the FBG flow sensor have a good linearity at flow-rate range from 5 to 20 ℓ/min and it appears that the available detectable range of the sensor is from 5 to 20 ℓ/min. As the applied current is high the FBG sensor exhibited high sensitivity. Fig 8 shows tunable spectral responses according to the gas flow-rates of the above 5 ℓ/min at the applied current of 100 ㎃. The spectral properties provide a clear shift.

From the curves of Fig. 8, we can distinguish two main regions in the flow sensing profile. One is Fig. 9, which shows non-linear characteristics at the low gas flow-rate with the range of less than 5 ℓ/min at two different currents of 100 and 120 ㎃. And another is Fig. 10, which shows linear characteristics at the high gas flow-rate with the range of more than 5 ℓ/min at two different currents of 100 and 120 ㎃. As a result, it is possible to measure the gas-flow rate in a range from 5 to 20 ℓ/min with a resolution of approximately 1 ℓ/min in a 10 ㎜ diameter flow line. Although there are shown results only with nitrogen gas, it is clear that the system could be employed to measure other kinds of gas flow-rates or to measure some other physical variables(temperature, strain, etc.). It is also possible to increase the sensor sensitivity and measurement range by changing dimensions of the sensor structure, the

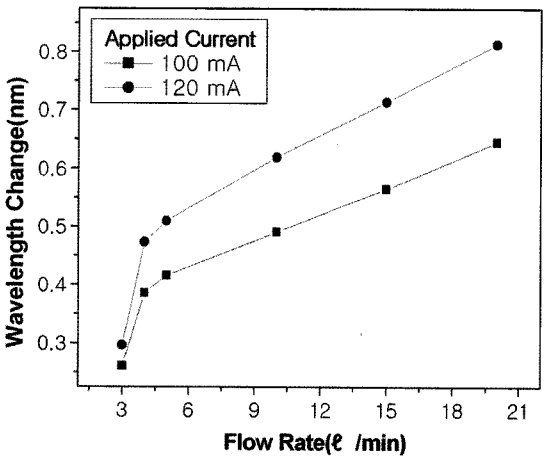

Fig. 7 Wavelength shift against the gas flow-rate in the range of 3ℓ/min to 20ℓ/min at two different currents of 100 and 120 ㎃.

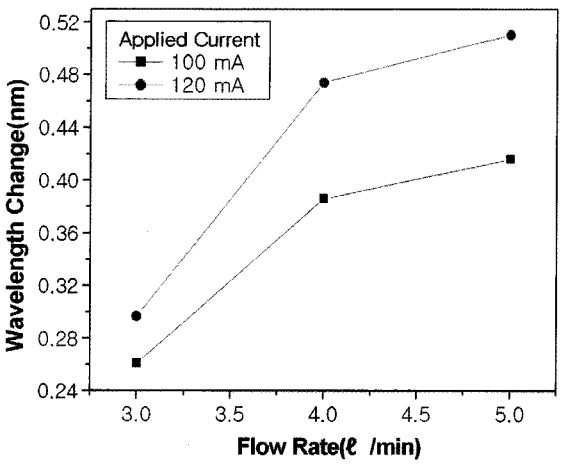

Fig. 9 Non-linear characteristics at the low gas flow-rate with the range of less than 5 ℓ/min at two different currents of 100 and 120 ㎃.

size of the flow line and the heating method. Table 2 shows values of wavelength change versus flow-rate and sensitivity for the applied currents of 100 and 120 ㎃. It is calculated by dividing the resonance wavelength range over the flow-rate range of 15. This method of calculation may be rough in nature but from the results obtained, all the relationships follow a quite good linearity which made it viable for such calculations to be supported in practice. The results also present that the characteristics of the higher applied currents offer the more sensitivity compared to those of the lower applied currents.

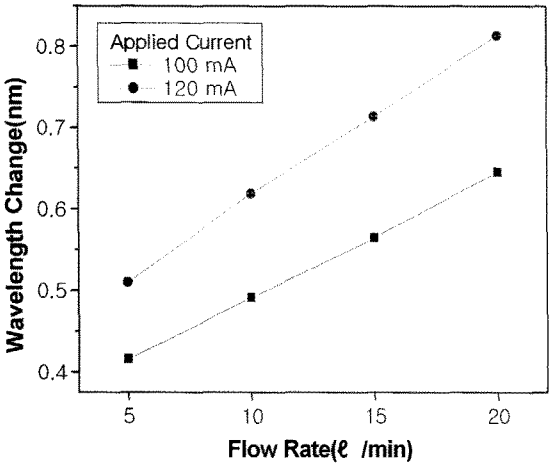

Fig. 10 Linear characteristics at the high gas flow-rate with the range of more than 5 ℓ/min at two different currents of 100 and 120 ㎃.

Table 2 Values of wavelength change versus flow-rate and sensitivity for the applied currents of 100 and 120 ㎃.

Flow Rate [ℓ/min]	Wavelength Change [nm]	
	[@Current=100㎃]	[@Current=120㎃]
5	0.4162	0.5102
10	0.4914	0.6193
15	0.565	0.7137
20	0.6456	0.8136
Sensitivity [pm/ℓ/min]	15.3	20.2

4. Conclusion

From the results obtained, we could obtain a correlation among wavelength change of the FBG sensor, the measured range of flow-rate and the applied current. It appeared that the characteristics below 5 ℓ/min are non-linear and those above 5 ℓ/min are linear at two different currents of 100 and 120 ㎃. As a result, it is possible to measure the gas-flow rate in a range from 5 to 20 ℓ/min with a resolution of approximately 1 ℓ/min in a 10 ㎜ diameter flow line. We can estimate that the available detectable range of the sensor is from 5 to 20 ℓ/min at 100 and 120 ㎃.

The FBG flow sensor presented in this paper has many advantages including passive nature, EMI immunity and capability of remote sensing. We try to apply this flow sensor to geophysical use because the advantages are leveraged in the application. By combining the flow sensor with FBG pressure and temperature sensors, FBG sensor system for pressure, temperature and flow measurement in a same package may be constructed. We believe with further research techniques and given more time, it can be analyzed and the results fully harnessed to produce useful applications in various fields of work and life.

Acknowledgement

This work was supported by the IT R & D program of MKE/IITA [2008-F-046-01, Development of core Technology of E-Narigation for IT Ship].

References

[1] Hung, S. T., Wong, S. C., and Fang, W.(2000), "The development and application of microthermal sensors with mesh-membrane supporting structure," Sensors and Actuators A, Vol. 84, pp. 70-75.

[2] Kaltsas, G., Nassiopoulos, A. A. and Nassiopoulou, A. G. "Characterization of a silicon thermal gas-flow sensor with porous silicon thermal isolation," IEEE Sensors J., Vol. 2, No. 5, pp. 463-475, Oct. 2002.

[3] Lin, G. C., Wang, L., Yang, C. C., Shih, M. C. and Chuang, T. J.(1998), "Thermal performance of metal-clad fiber Bragg grating sensors," IEEE Photon. Technol. Lett., vol. 10, no. 3, pp. 406-408.

[4] Lim, J., Yang, Q. P., Jones, B. E., and Jackson, P. R.(2001), "DP flow sensor using optical fiber grating," Sensors and Actuators A, Vol. 92, pp. 102-108.

[5] Nemoto, T., Hashimoto, Y., Sato, S. and Iitaka, H.(1998), "An optical fiber flow speed sensor of increased sensitivity," Elect. Eng. Jpn., pp. 1-8.

[6] Oda, S., Anzai, M., Uematsu, S., and Watanabe, K.(2003), "A silicon micromachined flow sensor using thermopiles for heat transfer measurements," IEEE Trans. Instrum. Meas., Vol. 52, No. 4, pp. 1155-1159.

[7] Okamoto, K., Ohhashi, T., Asakura, M., and Watanabe,

K.(1994), "A digital anemometer," IEEE Trans. Instrum Meas., vol. 43, no. 2, pp. 116-120.

[8] Shyu, C. T. and Wang, L.(1994), "Sensitive linear electric current measurement using two metal-coated single-mode optical fibers," J. Lightwave Technol., Vol. 12, No. 11, pp. 2040-2048.

[9] Svedin, N., Kalvesten, E., and Stemme, G.(2003), "A new edge-detected life force flow sensor," J. Microelectromech. Syst., Vol. 12, pp. 344-354.

[10] Wu, J. and Sansen, W.(2002), "Electrochemical time of flight flow sensor," Sensors and Actuators A, Vol. 97-98, pp. 68-74.

Received 12 December 2008
Revised 26 December 2008
Accepted 27 December 2008